

# THE 4TH INTERNATIONAL CONFERENCE ON ALUMINUM ALLOYS

## THE EFFECT OF ORIENTATION ON SHORT CRACK PATH AND GROWTH RATE BEHAVIOUR IN AL-LI ALLOY AA8090

P.A.S. Reed, I. Sinclair and P.J. Gregson

Dept. of Engineering Materials, University of Southampton, Highfield, Southampton, U.K.

### Abstract

The growth of physically short cracks at various orientations has been studied in a highly textured Al-Li alloy 8090. In comparison to the behaviour of long cracks at the same nominal  $\Delta K$ -levels the short crack specimens showed Stage I type macroscopically deflected crack growth at all  $\Delta K$  values. The TL long crack specimens showed this type of crack growth above  $\Delta K = 16-18$  MPa $\sqrt{m}$ . The slip-planes down which the Stage I type cracks grew were normally the "roof-top" planes of the brass-type texture. The L+30° orientation short crack specimen however also exhibited crack growth along the slip-plane common to both components of the brass type texture. The short crack specimens showed higher crack growth rates than the long crack TL orientation, but equivalent to the LT long crack specimen. There was little effect of short crack specimen orientation on crack growth rates, but striking differences in terms of crack path. It is proposed that the effect of crack path on lifing analyses in this material should be considered, as significant deflections in crack path can produce mixed mode loading conditions at the crack tip.

### Introduction

Al-Li alloys are widely recognised as offering appealing fatigue crack growth resistance characteristics, in addition to high specific strength and stiffness. The importance of microscopic crack *path* behaviour in controlling the fatigue resistance of Al-Li alloys has also been reported. The effects of macroscopic crack path deflection are rarely considered in lifing analyses for aircraft structures. Recent investigations of long crack growth in commercial damage tolerant Al-Li plate (AA8090) exhibiting a predominantly brass-type crystallographic texture have shown a preferentiality for slip band crack growth on a particular set of  $\{111\}$  plane orientations within the material [1,2]. This effect has been related to a combination of crack-tip stress/strain distribution and microstructural influences, rather than to the effect of crack-tip stress/strain fields alone. Work has been carried out on similar Al-Li plate in relation to the short crack/initiation regime. Different orientations have been examined, such that the preferred slip-planes experience different resolved shear stresses.

### Experimental

Simple bend bar specimens were produced from 28mm thick commercial AA8090 plate in the T8151 damage tolerant condition. Samples were cut from the central region of the plate and were established to have a predominantly brass type texture. The material's grain structure and directionality is shown in Figure 1a and in Figure 1b the pole figure for the centre region of the plate can be seen. In Figure 2 the orientations of the bend bars (TL, L+60° and L+30°) with respect to the rolling direction of the plate can be seen. Tensile specimens for the three different orientations were also tested.

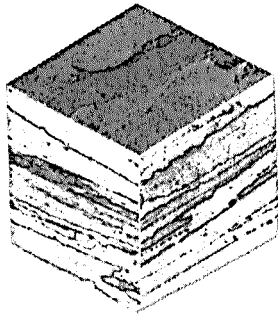


Figure 1a 8090 Plate Grain Structure

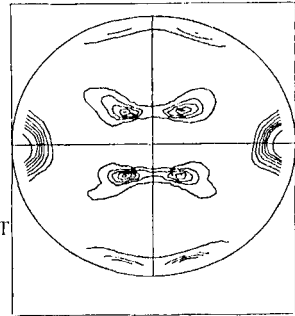
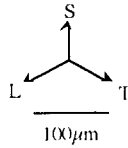


Figure 1b {111} Pole Figure for mid-thickness position

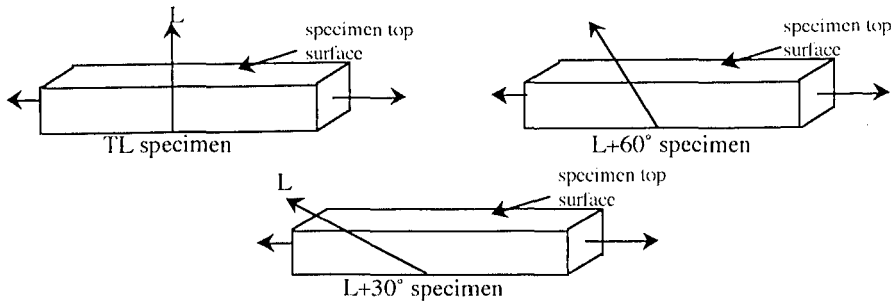


Figure 2 Specimen orientations with respect to rolling direction

The bend bar specimens had their top surfaces ground and polished to a  $1/4 \mu\text{m}$  finish and were then lightly etched in Keller's reagent to reveal the grain structure. Initially the specimens were tested at room temperature in air in four point bend. Fatigue testing at 20Hz and at a constant R-ratio of 0.1 was carried out on a 200kN Mand servohydraulic testing machine with Dartec computer control. The top surface maximum stress was 0.93 of the yield stress determined for each orientation. Cycling was halted every 10,000 cycles, and acetate replicas of the top surface were taken, thus providing a replica record of the crack initiation and growth. It was intended that all the specimens would be tested in this way, but apart from the TL orientation (in which crack initiation occurred after 200,000 cycles), no crack initiation was observed even after 400,000 cycles. Accordingly, it was decided to observe the short crack growth behaviour of these orientations by introducing a small corner notch in the central bend region of the specimen, using a razor blade. The notches produced in this manner were approximately  $700 \mu\text{m}$  (top surface) by  $400 \mu\text{m}$  (side surface). The crack growth data relating to initial crack growth from the notch up to ~ four times the notch width from the razor cut tip was discarded due to the possible influences of residual stress associated with the deformation around the cut, and the "bluntness" of the cut. The top surface maximum stress for the notched specimens was also kept at 0.93 of the yield stress. The  $a$  versus  $N$  data for these cracks were calculated from the replica record. The projected crack length, perpendicular to the applied tensile stress, was measured, so that the  $da/dN$  data in that direction could be calculated, and compared with equivalent long crack growth behaviour. A number of assumptions were made, chiefly that the corner crack shape could be approximated to a planar crack in order to calculate  $\Delta K$  values at the top surface using Pickard's analysis (3). Pickard has defined  $K$  for corner cracks as:

$$K = M_G M_B M_S F(\sigma) \Phi (\pi a)^{1/2}$$

where  $M_G$ ,  $M_B$  and  $M_S$  are correction factors, dependent on specimen geometry and crack length,  $F(\sigma)$  is the complex stress function, calculated by FEM but approximated by a polynomial expression,  $\Phi$  is the ellipticity correction factor and  $a$  is the crack dimension in question.

Conventional long crack growth data has also been obtained for the plate material, using both CCT and SENB specimens (in four point bend). The TL and LT orientations were tested at 20Hz, at room temperature in air at an R-ratio of 0.1. The tests were carried out under constant load range (increasing  $\Delta K$  conditions). Crack growth was continuously monitored using a pulsed four point probe potential drop method. The fatigue fracture surfaces of all the specimens were also studied in a JEOL 300T SEM operating at 25kV.

### Results and Discussion

Tensile behaviour. The following variation in tensile properties with orientation was observed:

Table 1 - Variation of tensile properties with orientation

Orientation s	Yield Stress (MPa)	UTS (MPa)	% elongation to failure
TL	412	470	2.3
L+30°	320	452	4.4
L+60°	290	446	6.5
LT	389	479	6.0

These variations in tensile properties are comparable with various results given in the literature for similar Al-Li materials (4). In Figure 3 the  $\{111\}$  slip plane orientations associated with the two individual crystallographic components which make up the overall brass-type texture can be seen for the TL orientation.

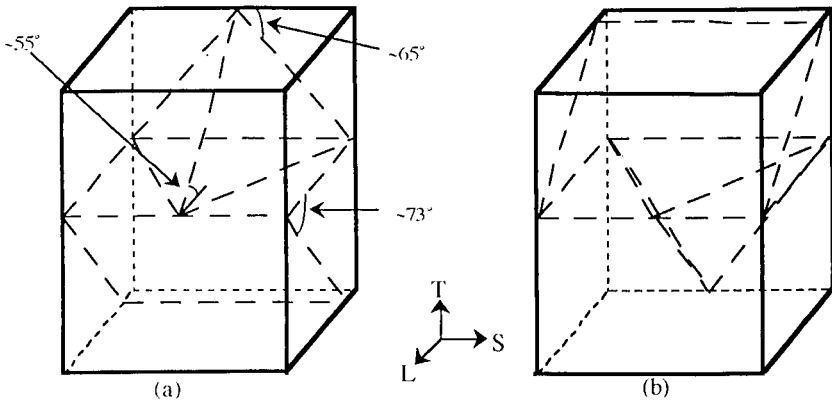


Figure 3  $\{111\}$  slip-planes associated with the two crystallographic orientations making up the brass-type texture

In terms of Figure 3 (a) it may be seen that there are a pair of planes angled to the plate through-thickness direction (described here as 'roof-top'), and a pair of planes parallel to the through-thickness direction (described here as 'flat'). The second grain orientation shown in Figure 3 is

simply a mirror image of the first through the LS plane, in keeping with the symmetry of the rolling process. It may be seen that the  $\{111\}$  plane orientation lying parallel to the LS plane is unique in being common to both crystallographic variants of the brass texture. In the  $L+30^\circ$  and  $L+60^\circ$  specimens the slip-planes will have been rotated with respect to the tensile axis, and the resolved shear stresses might be expected to vary accordingly.

### Fatigue behaviour

Figure 4a

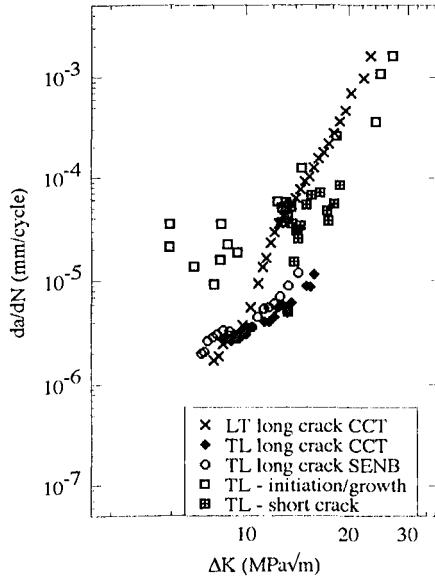
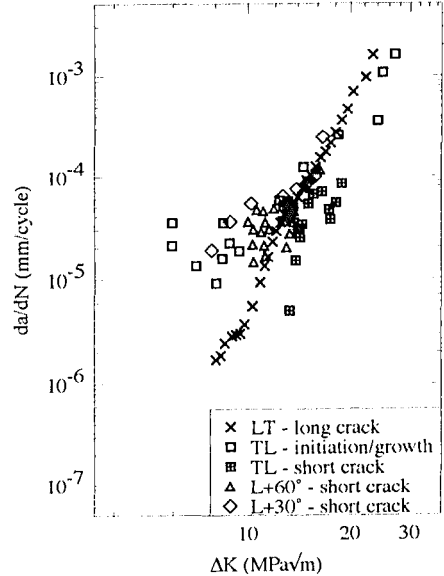


Figure 4b



**Long crack behaviour.** Fatigue crack growth data are presented for both the long crack and short crack specimens in Figures 4a and b. In Figure 4a the long crack data for both specimen types and orientations can be compared. The long crack growth rate data for CCT and SENB specimen types in the TL orientation are clearly comparable. The TL long crack data, which has been obtained under increasing  $\Delta K$  conditions, only extends over a decade of  $da/dN$  values and up to  $\sim 16$ – $18$   $MPa\sqrt{m}$ , above this point significant macroscopic crack deflection at  $\sim 60^\circ$  to the nominal crack growth direction occurs and the calibration for the potential drop crack monitoring method can no longer be used. The LT orientation shows crack growth rates similar to the TL orientation at low  $\Delta K$  levels but at higher  $\Delta K$ -levels the data start to diverge, and far faster crack growth rates are seen, up to a factor of six times faster than the TL orientation over the majority of the  $\Delta K$  range. The LT data are collected over a much wider  $\Delta K$  and  $da/dN$  range, in this case no macroscopic crack deflection occurs although microscopic crack deflections are common. In both cases, at  $\Delta K$ -values of less than  $\sim 12$   $MPa\sqrt{m}$ , crack growth along a mixture of  $\{001\}/\{111\}$  slip-planes has been observed, at higher  $\Delta K$  values and during macroscopically deflected crack growth, crack growth occurs predominantly along  $\{111\}$  type planes, (1).

**Short crack behaviour.** The TL orientation “notched” and freely initiated short crack growth behaviour is also plotted in Figure 4a and compared with the long crack data. The two sets of data exhibit a high degree of scatter, but the “notched” data appears to show lower  $da/dN$  values for the same nominal  $\Delta K$  levels. It appears that the “notching” has to some extent affected the subsequent growth behaviour of the small cracks, compared with the growth behaviour of freely initiating small cracks. The TL “notched” short crack data shows “classic” acceleration and

deceleration behaviour, often associated with the crack encountering microstructural barriers (5,6) e.g. grain boundaries, in a wide variety of materials. The periodicity of the temporary arrests is, however, too great to be simply linked to grain boundary arrests of the crack. The growth rates observed for the short cracks are up to an order of magnitude greater than those found for the long crack TL orientation, at the same nominal  $\Delta K$  levels. Compared with the LT long crack data, at higher  $\Delta K$  levels similar  $da/dN$  rates are seen. In Figure 4b, the three orientations tested in the short crack configuration are compared with the LT long crack data. There appears to be little effect of orientation on short crack growth rates, this is in stark contrast to the marked effect of orientation on long crack growth rates.

It is important to remember that the short crack  $da/dN$  and  $\Delta K$  data were all calculated for *projected* crack lengths, perpendicular to the applied tensile stress. The use of  $\Delta K$  in correlating long crack and short crack behaviour is generally accepted as a means of comparing behaviour, but there are clearly inherent problems in using a parameter based on LEFM assumptions for the short crack case, where crack lengths are small compared with crack tip plasticity. The simplistic assumptions, based on projected crack length, made in calculating  $\Delta K$  for short cracks are also generally acknowledged. In Figures 5a-c, overviews of the short crack specimen fatigue fracture surfaces are shown, the polished top surface of the specimens can be seen, and the initiation site is arrowed in each case. It is clear that extremely tortuous and macroscopically deflected crack growth is observed for all orientations of short crack specimen, with perhaps the L+30° short crack specimen showing the least "deflected" behaviour. Under these conditions it is clear that the simple assumptions used in calculating  $\Delta K$  mean that this value does not really represent the local crack tip stress or strain conditions (the basis for its use in comparing  $da/dN$  rates for cracks of different size). In the long crack case, where LEFM conditions do hold, and for pre-deflection crack growth, then  $\Delta K$  can be considered to characterise the crack growth conditions successfully.



Fig. 5a TL specimen



Fig. 5b L+60° specimen



Fig. 5c L+30° specimen

### Fractography

The *deflected* crack growth observed in the TL long crack specimen occurs predominantly along the so-called roof-top planes. In the LT long crack specimen the crack does grow along these planes but they are at a lesser angle to the nominal crack path, and it zig-zags with no overall macroscopic deflection. The marked difference in crack growth rates is considered to be due, in part, to a smaller effect of shielding in this orientation compared with the TL orientation. The

slip-planes along which crack growth has occurred in the short crack specimens can be established by inspection of the fracture surface facets formed by fatigue crack growth. In the TL orientation, both the freely initiating crack and the short crack initiated by a razor cut were macroscopically deflected (e.g. Figure 5a). Crack growth has occurred predominantly down the roof-top slip plane, in a manner analogous to the long crack macroscopically deflected crack growth. In the L+60° short crack specimen, although there is evidence of some crack path tortuosity, the fracture surface is not so macroscopically faceted, there are some signs that the roof-top planes are again preferred (ridges running down the specimen as shown by arrows in Figure 5b). This specimen orientation has not shown the high levels of crack deflection observed in the other two short crack orientation specimens. All these specimens showed temporary decelerations of crack growth, this can now be understood in terms of the macroscopic tortuosity of the crack path, and the varying surface roughness induced closure effects associated with this.

The L+30° short crack specimen has a "prism-like" fracture surface (Figure 5c). The crack has been initiated at the top left-hand corner by a razor cut, and the resulting corner crack seems to have grown along a roof-top plane at the side of the specimen and along the "common" {111} slip-plane (which is shared by both variants of the brass type texture) along the top surface. At approximately the mid-point of the specimen width, the crack deflects *back* along the complementary roof-top plane, forming a "prism-like" fatigue fracture surface. Closer observation of the L+30° top surface, shows that microscopically, the top surface crack does show minor deflections (Figure 6a), but that the fatigue fracture surface shows typical {111} slip-plane dominated crack growth (Figure 6b). Similar microscopic crack growth modes are observed for the TL and L+60° specimens (Figures 6c and d).

The comparison of "long" and "short" crack growth rates in this alloy must take into account the different crack propagation modes. The long crack data is all pre-deflection data or data obtained when microscopic, rather than macroscopic, deflections are occurring and the crack is growing nominally perpendicular to the applied tensile stress. At higher  $\Delta K$  levels (16-18 MPa $\sqrt{m}$ ) in the TL orientation the crack deflects along the roof-top {111} slip planes, exhibiting a Stage I like behaviour. The short crack specimens all show macroscopically deflected, Stage I type behaviour from the start of crack growth, with *projected* crack lengths used to calculate  $da/dN$  and  $\Delta K$  values. The levels of shielding associated with this highly faceted, macroscopically deflected crack growth mode will be due to the decrease in crack driving force due to the deflected nature of the crack (7) as well as due to surface roughness induced closure effects. It is generally considered (8) that the difference observed between short crack and long crack behaviour in this alloy can be linked to the restricted crack tip shielding associated with small flaws of limited wake. The short crack specimens, showing such macroscopically deflected crack growth, at longer crack lengths (i.e. higher  $\Delta K$  levels) will experience greater shielding effects than the LT specimen at a similar nominal  $\Delta K$  level. The  $da/dN$  values are however quite similar.

In comparing the relative short crack behaviour of the different orientations, little difference is observed in terms of data calculated from projected crack lengths, but in terms of crack path, there are clear effects of orientation. A deflected crack, growing at any angle other than perpendicular to the mode I loading direction, will be experiencing mixed mode loading conditions. It has been shown (9) in this material, that crack growth rates for macroscopic mixed mode crack propagation are markedly higher than those under nominal mode I loading conditions.

### Summary and Conclusions

Short crack specimens of different orientations have been tested and compared with long crack specimens in AA8090 alloy at  $R = 0.1$ . The TL long crack specimens exhibit Stage I like macroscopically deflected crack growth at  $\Delta K$  levels of 16-18 MPa $\sqrt{m}$  and above, the deflection is at approximately 60° to the nominal crack growth direction for the TL orientation, and at approximately 35° for the LT, where only microscopic deflection is observed. The cracks grow along the so-called "roof-top" planes of the brass-type texture. The effect of orientation on

Direction of crack growth in all specimens

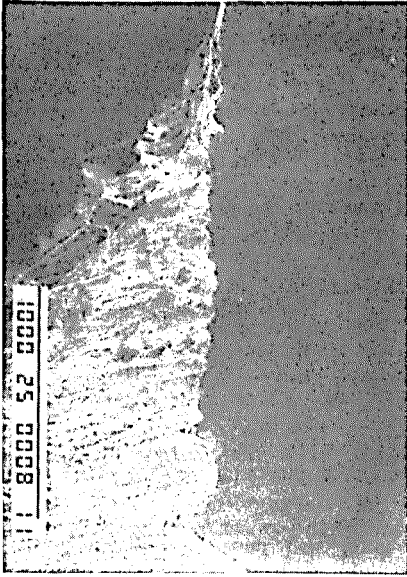


Figure 6a L+30° top surface, showing minor deflections



Figure 6b Close-up of L+30° facet, showing {111} dominated crack growth mode



Figure 6c Typical TL fatigue surface

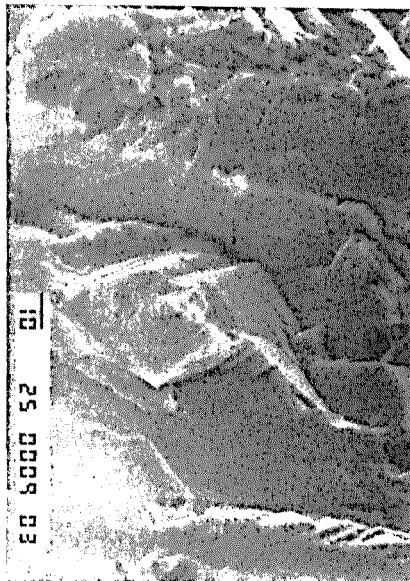


Figure 6d Typical L+60° fatigue surface

apparent  $da/dN$  values at equivalent  $\Delta K$ -levels is marked, with the LT specimen showing far higher crack growth rates than the TL orientation at  $\Delta K$  levels of about 12 MPa $\sqrt{m}$  and above.

Three short crack orientations have been studied: TL, L+30° and L+60°. The short crack specimens have exhibited Stage I type, macroscopically deflected crack growth at all nominal  $\Delta K$ -levels. In the TL and L+60° specimens crack growth occurred principally along the roof-top planes, in the TL orientation this gave extremely deflected crack growth. The L+60° specimen had the lowest yield stress and UTS, but highest % elongation to fracture of all the orientations. The L+30° specimen had crack growth along the roof-top planes, but also along the common plane (shared by both components of the brass texture). The reason for the change in favoured slip-plane with orientation is not clear, and will require some analysis of the crack-tip stress field and the manner in which the resolved stresses and strains act upon these slip-systems in the different orientations. There was no apparent effect of orientation on  $da/dN$  values, although the crack paths varied. The  $da/dN$  values were of the same order as those observed for the LT long crack specimen, but up to an order of magnitude greater than those observed for the TL long crack specimen. A short crack effect is observed in this material, but more importantly, a very deflected crack path is observed, analogous to the macroscopically deviated crack path behaviour of the long crack specimens. Some account of crack path must be made in lifing analyses, if the crack path is very deflected, mixed mode loading conditions are experienced by the crack tip, and there is evidence that such cracks can grow very much faster than a crack growing under equivalent mode I loading conditions. Incorporating such considerations in lifing analyses of 8090 alloy for airframe applications is clearly important.

#### Acknowledgements

Thanks are due to Prof. A.F.W. Willoughby for the provision of laboratory facilities at the Dept. of Engineering Materials, University of Southampton and to A. Hobson and W.S. Tee who carried out the mechanical testing reported in this paper.

#### References

- (1) I. Sinclair and P.J. Gregson, Fatigue 93, Proc. 5th Intl. Conf. on Fatigue and Fatigue Thresholds, eds. J.P. Bailon and J.I. Dickson, Warley : EMAS, Vol. 2, (1993) 635
- (2) I. Sinclair and P.J. Gregson, to be published
- (3) A.C. Pickard, The application of 3D finite element methods to fracture mechanics and fatigue life prediction, (EMAS, Cradley Heath, 1986)
- (4) A.W. Bowen, Mater. Sci. Tech., 6, (1990), 1058
- (5) J. Lankford, Fatigue Fract. Engng Mater. Struct., 8, (1985), 161
- (6) D. Taylor and J.F. Knott, Fatigue Engng Mater. Struct., 4, No.2, (1981), 147
- (7) S. Suresh and C.F. Shih, Int. J. Fract., 30, (1986), 237
- (8) K.T. Venkateswara Rao and R.O. Ritchie, Int. Met. Rev., 37, (1992), 153
- (9) I. Sinclair and P.J. Gregson, Scripta Met. et Mat., 30, (1994), 1287